The 14th World Conference on Earthquake Engineering
October 12-17, 2008, Beijing, China

CRACK DAMAGE DISTRIBUTION OF CONCRETE FILLED STEEL TUBE FRAME UNDER EXTREMELY STRONG GROUND MOTION

Motoo SAISHO

Professor, Dept. of Architecture, Graduate School of Science and Technology, Kumamoto Univ., Kumamoto, Japan
Email: saisho@gpo.kumamoto-u.ac.jp

ABSTRACT:
Seismic response and crack damage of concrete filled steel tube frame (CFT-frame) under strong ground motion are numerically analyzed and the damage ratio and damage distribution in the frame are investigated. In order to prevent the damage concentration, the design condition of CFT-frame expressed by the strength ratio of concrete to steel tube is derived from the numerical results of seismic response and damage ratio distribution. CFT-frames are designed on the basis of the proposed design condition and the calculations of the seismic response and damage of them have been carried out. From the calculated results, it is ascertained that the proposed design condition of CFT-frame is useful to prevent the damage concentration in CFT-frame under strong ground motion.

KEYWORDS: *concrete filled steel tube, seismic response analysis, accumulated plastic deformation, steel tube crack, damage ratio.*

1. INTRODUCTION

Seismic response collapse of concrete filled steel tube frame (CFT-frame), which is composed of CFT-column and H-section beam, is closely related to the fracture of CFT-column caused by the steel tube crack[1)-3)]. Especially the first crack fracture of CFT-column among all CFT-column fractures in the frame is directly related to the seismic response collapse of CFT-frame. From this reason it is required in the ultimate earthquake resistant design of CFT-frame to prevent the damage concentration of CFT-column.

The main conditions of ultimate earthquake resistant design of multi-story CFT-frame are the story shear strength and the distribution condition of it. But the crack fracture of CFT-column under seismic load can not be prevented only by making the story shear strength of frame large enough because the crack fracture of CFT-column is effected by the strength ratio of filled concrete to steel tube of it[4)]. To prevent the fracture damage concentration of CFT-frame, the design condition expressed by the strength ratio of filled concrete to steel tube of CFT-column is required.

On the basis of numerical analysis of seismic response damage of multi-story CFT-frame, the fracture damage ratio of CFT-column and the damage distribution of CFT-frame are investigated and the optimum design condition to prevent the fracture damage concentration of CFT-column are derived from the numerical results.

2. NUMERICAL ANALYSIS METHOD OF SEISMIC RESPONSE AND DAMAGE DISTRIBUTION

2.1 Multi-story CFT-frame model

In the dynamic collapse analysis of CFT-frame[1)-3)], the multi-story plane frame is assumed to be composed of the rigid panel zones of beam-column connection and the axially elastic members with elastic-plastic hinges at the both ends as explained in Fig.1. The mass of frame is concentrated in every panel zone of beam-column connection and the rotational inertia of it is determined by assuming the mass in the panel zone distributes uniformly.

The deformation of frame is expressed by the rotation (θ_I, I: number of beam-column connection), the horizontal displacement (u_I) and the vertical displacement (w_I) of every rigid beam-column connection. The viscous damping of frame is expressed by the Rayleigh Damping in which the damping factors of the first mode (h_1) and the second mode (h_2) are assumed to be h_1=0.02 and h_2=0.02.

2.2 Restoring force characteristics and model of CFT-column

The restoring force model of elastic-plastic hinge was determined on the basis of the dynamic loading test of CFT-column[5)-6)]. Fig.2 shows how to define the restoring force (M) and the deformation ($\phi(=\delta_c/L_c)$) by the horizontal load (H), the axial load (N) and the column-end deflection (δ_c) of test.

According to the test results the restoring force divided by M_u (M/M_u) of CFT-column until the local buckling of steel tube is approximated by the Bi-linear model whose skeleton curve is explained in Fig.3(A) and after the local buckling of steel tube it is expressed by the Clough model[8)] as shown in Fig.3(B). The stiffness ratios in the plastic

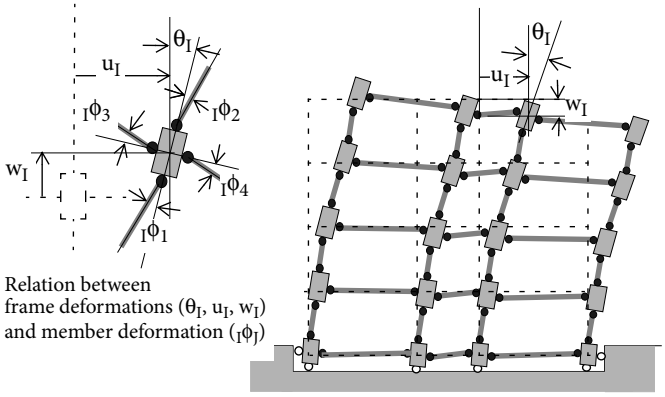

Fig.1 Frame model of numerical analysis

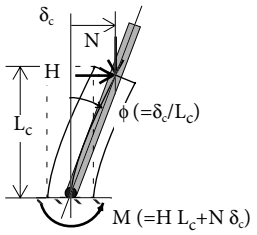

Fig.2 Loads of CFT-column (H, N) and restoring force (M) of fixed-end

range in Fig.3(A) and Fig.3(B) are given as K_1/K_0=0.2, K_2/K_0=0.001 which are approximated on the basis of the test result.

The restoring force model mentioned above is defined by the restoring force divided by M_u (M/M_u) in which the ultimate bending strength M_u changes at every moment according to the varying axial force of CFT-column. From this reason the restoring force model presented here can simulate the effect of varying axial force of CFT-column.

2.3 Local buckling and crack fracture of CFT-column

From the cyclic loading test of CFT-column it is shown that the steel tube of CFT-column cracks and fractures when the accumulated plastic strain of steel tube becomes to be equal to the critical value ($\alpha\varepsilon_f$). From this result the crack and fracture condition of CFT-column is expressed by Eq.(1)[5)-6)].

$$\Sigma\varepsilon_{TC}+\Sigma\varepsilon_T = \alpha\varepsilon_f \quad (1)$$

in which ε_T is the plastic tension strain of steel tube in the tension stress side and ε_{TC} is the plastic strain due to the local buckling deformation of steel tube in the compression stress side as explained in Fig.5. In Eq.(1), α (=-0.3ρ+5.0): constant expressed by the strength ratio of concrete to steel tube (ρ), ε_f: fracture strain, Σ: summation of plastic strain under cyclic load. From Eq.(1) the damage ratio of steel tube ($_cD_{cr}$) is expressed by Eq.(2).

$$_cD_{cr} = (\Sigma\varepsilon_{TC}+\Sigma\varepsilon_T)/\ \alpha\varepsilon_f \quad (2)$$

The local buckling of steel tube in the calculation of ε_{TC} is obtained by the upper bound theorem of the limit analysis[7)]. By the use of Eq.(1) and Eq.(2), the local buckling and the crack of steel tube in the restoring force of CFT-column are decided and it is assumed that the restoring force and the stiffness of CFT-column are fully lost after the steel tube crack.

2.4 Restoring force model and crack fracture of H-section beam

The H-section beam of multi-story CFT-frame is also expressed by the elastic member with the elastic-plastic hinges at both ends as shown in Fig.1. The restoring force of the elastic-plastic hinge is decided by the Bi-linear model shown in Fig.4 in which the restoring force characteristics are given by the full plastic moment (M_p) and the ultimate bending strength ($_bM_u$) of H-section beam. The strain hardening of behavior H-section beam is approximated by Eq.(3) which is obtained by assuming the H-section beam is expressed by the two-flange section member.

$$\frac{K_1}{K_0} = \frac{1/y - 1}{1.5y(1-y)(1+u)-1} \quad (3)$$

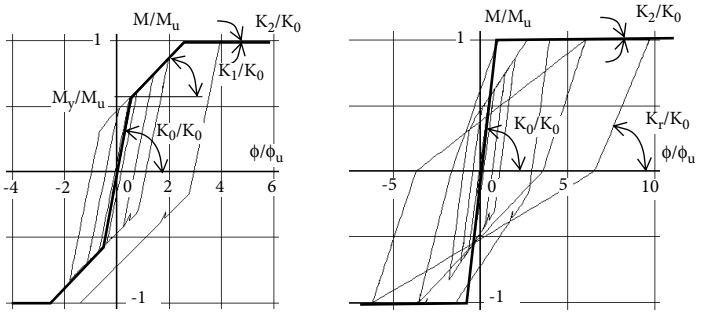

(A) Bi-linear model and skeleton curve (K_1/K_0=0.2, K_2/K_0=0.001)

(B) Clough model and skeleton curve (K_2/K_0=0.001, K_r/K_0: unloading stiffness ratio

Fig.3 Restoring force model and skeleton curve of CFT-column

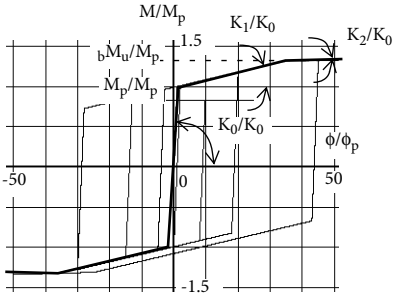

Fig.4 Bi-linear model and skeleton curve of H-section steel beam
(K_1/K_0 : Eq.(3), K_2/K_0=0.001, $\phi_p=M_p/K_0$)

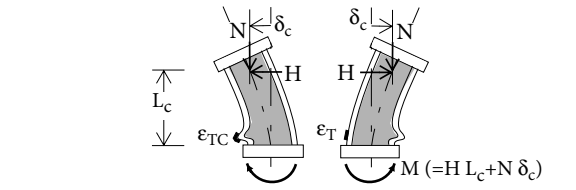

Fig.5 Load, deformation and plastic strain of CFT-column

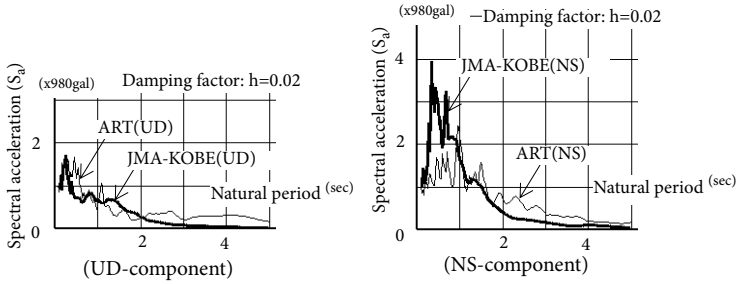

Fig.6 Response spectra of strong ground motions used in numerical analysis of CFT-frame

in which y(=σ_y/σ_u) and u(=$\varepsilon_u/\varepsilon_y$) mean the yield stress ratio and the ultimate tensile strain ratio respectively.

The crack fracture of H-section beam[3] is assumed to be the very low-cycle fatigue behavior and to be approximated by the Palmgren-Miner rule[9]. From the Palmgren-Miner rule that the damage ratio of H-section beam is given by the accumulation of the damage in each cycle, the damage ratio at any moment under cyclic load can be expressed by Eq.(4) in which N_{fj} means the number of cycle to fracture under the j-th cycle load.

$$ {}_bD_{cr} = \sum_j \frac{1}{N_{fj}} \qquad (4) $$

The number of cycle to fracture N_f in Eq.(4) is approximated by the Coffin-Manson expression[9] in Eq.(5).

$$ \varepsilon_{pa} = \varepsilon_f (2N_f)^c \qquad (5) $$

in which ε_f: fracture strain and ε_{pa}: plastic strain amplitude of H-section beam.

2.5 Strong ground motion

To calculate the seismic response and damage of CFT-frame, JMA-KOBE NS & UD (1995) recorded in Kobe and the artificial ground motion ART NS & UD are used as input ground motion. The acceleration response spectra (S_a) of them are shown in Fig.6 comparing with each others. In order to investigate the effect of the characteristics of ground motion, the ground motions satisfy the conditions that the spectrum intensities (SI) of them are the same and the response spectra are quite different between them as shown in Fig.6.

3. DESIGN OF MULTI-STORY CFT-FRAME

3.1 Design conditions of CFT-frame

The CFT-frames to be calculated in this study are composed of CFT-columns and H-section beams and designed under the following conditions[3].

i) According to the Japanese design code, the ultimate base shear strength ratios (C_B) of the 15-story 3-bay frames and the 7-story 3-bay frames are C_B=0.25 and C_B=0.40 respectively. The ultimate strength of frame is calculated by the limit analysis assuming the collapse mechanism of frame with plastic hinge at every beam-end and the upper and lower column-ends in the top story and the first story.

ii) The column-over-design factors (r_c) of all stories except the highest story are the same in each frame. There are three kinds of factors and they are r_c=1.2, r_c=1.5 and r_c=2.0.

iii) The strength ratios of filled concrete to steel tube ρ (=$\sigma_c A_c/\sigma_u A_s$, A_c, A_s: sectional areas of concrete and steel tube respectively) of all CFT-columns are assumed to be the same in each frame. In considering with the range of test data (ρ<3.4) the strength ratio of CFT-column is ρ<5.0.

iv) Every H-section beam of multi-story frame satisfies the critical conditions of the width-to-thickness ratio of flange (b/t_f) and web (h/t_w) and the lateral buckling length ($L_b h/A_f$). They are b/t_f=20, h/t_w=71 and $L_b h/A_f$=375.

3.2 Designed CFT-frames

Multi-story CFT-frames analyzed in this study are 15-story 3-span frame and 7-story 3-span frame. Assuming that any section of steel tube are available, they are designed under the conditions mentioned above.

The story-height of every CFT-frame is 4.0 m and the span lengths of outer span and inner span are 8.0 m and 6.0 m respectively. The weight of each story is 2000KN. The yield stress (σ_y) and tensile strength (σ_u) of steel tube and H-section beam are σ_y=340N/mm^2, σ_u=440N/mm^2. The fracture strains (ε_f) of steel tube and H-section beam are the same and it is ε_f=0.2. The compression strength of concrete (σ_c) filled in steel tube are σ_c=30N/mm^2, 60N/mm^2 and 120N/mm^2.

The designed all CFT-frames are shown with white circles in Fig.7 in which there are the diameter (D) of CFT-column in the first story and the natural period (T) of CFT-frame. In account that the design conditions of CFT-frame are quite different among them, every diameter of CFT-column (D) is in practical range and the natural peri-

ods (T) of 15-story frame and 7-story frame are nearly constant respectively. From these designed frames it is ascertained that the design method of multi-story CFT-frame shown in the former section is useful.

4. DAMAGE CONCENTRATION OF CFT-FRAME

The damage distributions of CFT-frame under JMA-KOBE NS&UD and ART NS&UD are shown in Fig.8(A) and Fig.9. The damages of CFT-frame shown in these figures are the crack fracture ratio of CFT-column ($_cD_{cr}$) and H-section beam ($_bD_{cr}$) explained in section 2.3 and section 2.4. In Fig.8 the damage ratios are expressed by the thick lines perpendicular to the axis of column and beam. The thick lines are also explained by the numerals in the figures. Fig.9 shows the seismic response damages of all CFT-frames shown in Fig.7. In Fig.8(A) and Fig.9 we can see the remarkable differences of damage concentration among the CFT-frames and the remarkable concentration of damage ratio in some CFT-frames in spite that all CFT-frames shown in these figures are designed under the same design condition of ultimate story shear strength and strength distribution along the story. From these results it is also ascertained that the damage concentration can not be prevented only by the design conditions of story shear strength or distribution of it.

5. DESIGN CONDITION TO PREVENT DAMAGE CONCENTRATION

5.1 Accumulated plastic deformation of CFT-column

According to cyclic loading test of CFT-column, the crack fracture of CFT-column is closely related to the accmulated plastic deformation of it[5)-6)]. From this reason, the distributions of the accumulated plastic deformation in numerically analyzed CFT-frames under strong seismic load are examined and some of the results are shown in Fig.10. The thin real lines are numerically analyzed seismic responses and the thick real lines show the approximations expressed by the sum of the natural deformations (P_i) given by Eq.(6).

$$P_i = \sum_{m} C_m \left(\frac{{}_m\phi}{\phi_u}\right)_i \qquad (6)$$

in which $\phi_u=M_u/K_o$, M_u: ultimate bending moment, K_o: initial bending stiffness, $_m\phi$: CFT-column deformation

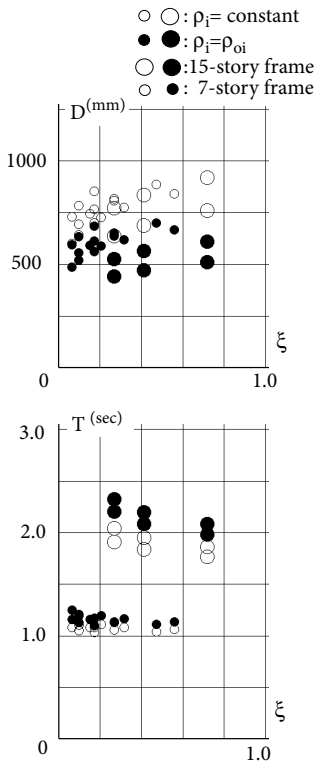

Fig.7 Diameter of CFT-column (D) and natural period (T) of CFT-frame

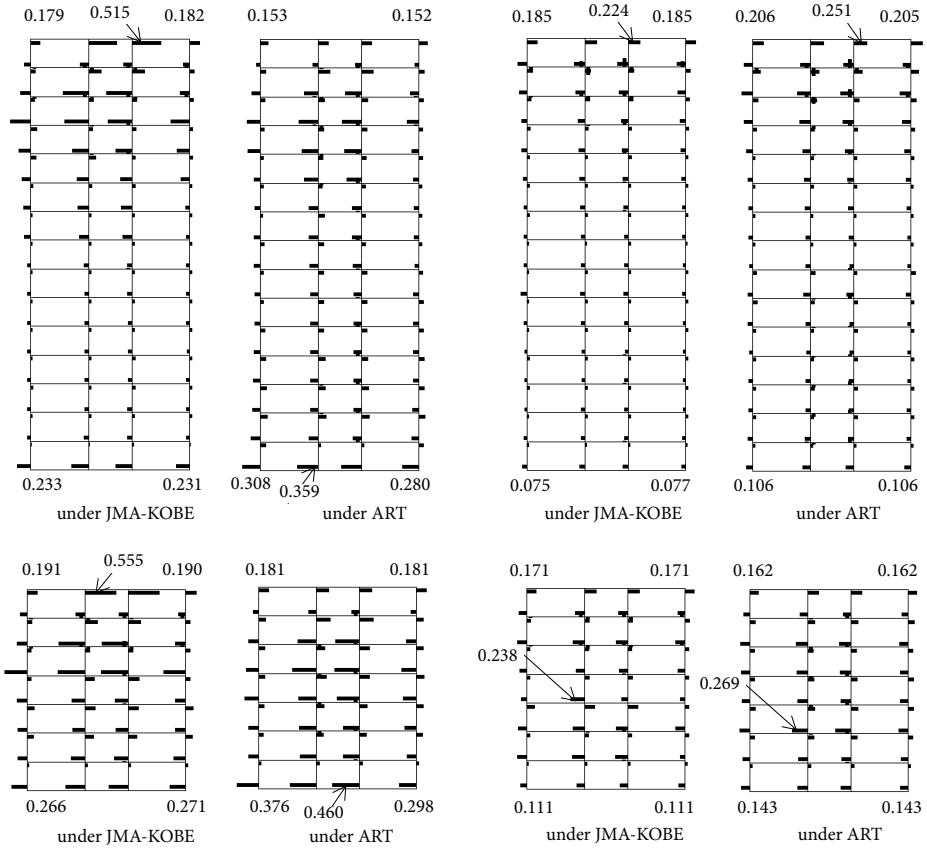

(A) CFT-frames designed under ρ_i=5.0
(r_c, ρ_i, σ_c)=(1.5, 5.0, 60N/mm^2)

(B) CFT-frames designed under ρ_i= ρ_{oi}
(r_c, ρ_i, σ_c)=(1.5, ρ_{oi}, 60N/mm^2), $(\rho_{oi})_{max}$=5.0

Fig.8 Seismic response damages of CFT-frame ($_cD_{cr}$, $_bD_{cr}$)

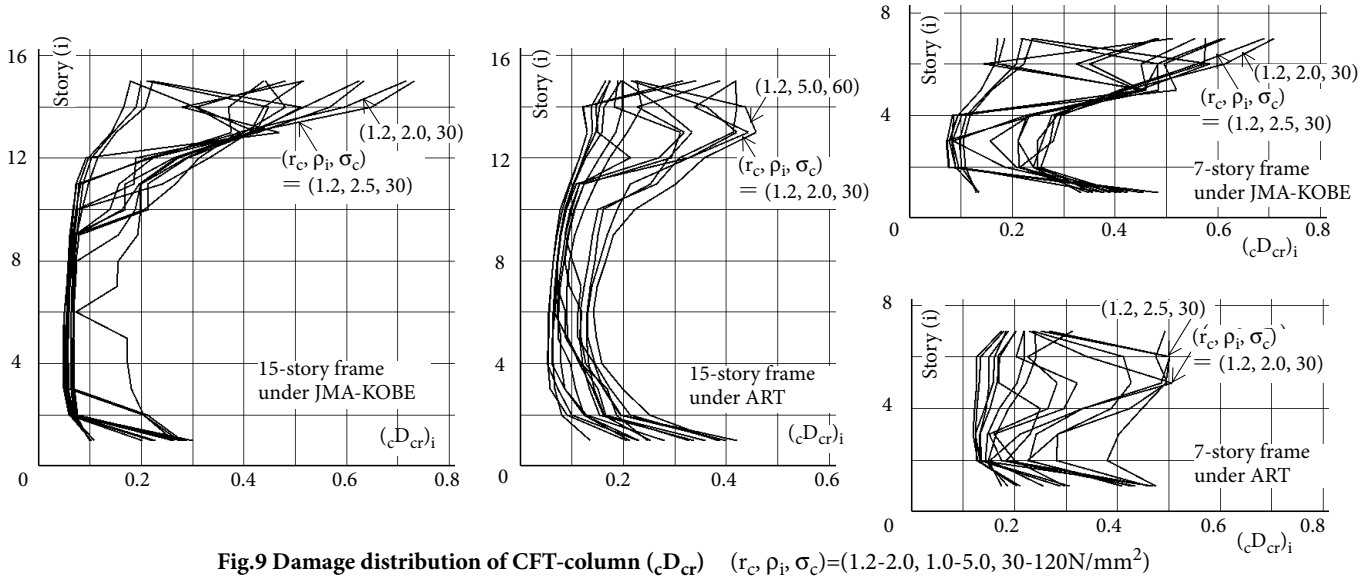

Fig.9 Damage distribution of CFT-column ($_cD_{cr}$) (r_c, ρ_i, σ_c)=(1.2-2.0, 1.0-5.0, 30-120N/mm^2)

by natural frame deformation, m: order of natural frame deformation, C_m: constant, i : number of story. The dashed lines show the natural deformations included in the thick real line. We can see that Eq.(6) gives the good approximation of the accumulated plastic deformation of CFT-column.

To apply the approximated distribution of accumulated plastic deformation of CFT-column to design condition of CFT-frame, the average values of all CFT-frames are calculated and shown in Fig.11. The obtained values, which are designated by P_{oi} in Fig.11, express the maximum value among the accumulated plastic deformations of all column-ends in each story.

5.2 Plastic tension strain components of CFT-column

As mentioned in Eq.(2), the fracture damage ratio of CFT-column is given by the two components of $\Sigma\varepsilon_{TC}/(\alpha\varepsilon_f)$ and $\Sigma\varepsilon_T/(\alpha\varepsilon_f)$. The time histories of the component in seismic response of CFT-frame are shown in Fig.12. It is shown in this figure that the two components and the time histories of them are similar between them. According

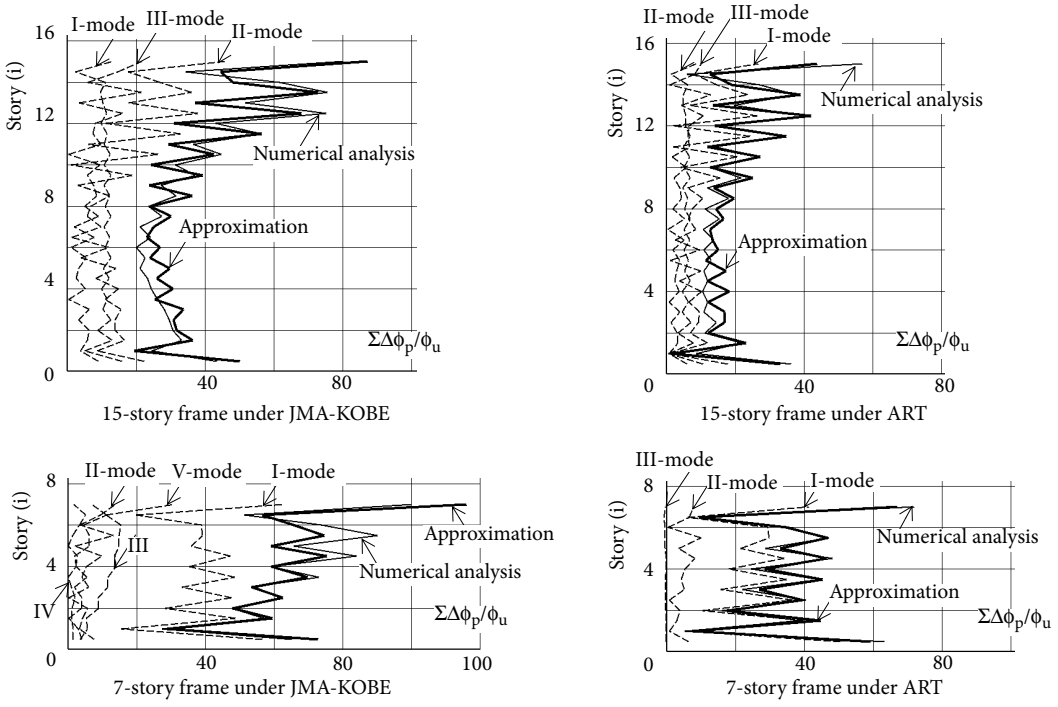

Fig.10 Accumlated plastic deformation of CFT-column and approximation by natural deformation of CFT-frame (r_c, ρ_i, σ_c)=(1.2, 5.0, 60N/mm^2)

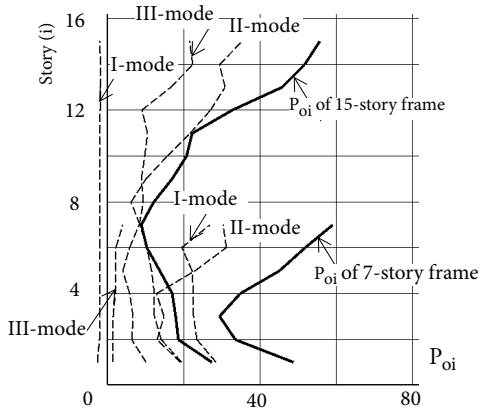

Fig.11 Approximeated distribution of accumulated plastic deformation (P_{oi})

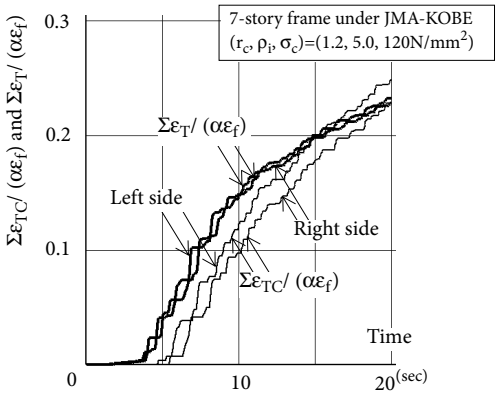

Fig.12 Time histories of damage ratio components of CFT-column under strong seismic load

to the design condition and the input ground motion, the differences between the two components changes but the time histories of them are similar to that in Fig.12. From this reason it is assumed here that the damage ratio can be approximated only by the plastic strain in the tension stress side ($\Sigma\varepsilon_T$) as shown in Eq.(7).

$$ {}_cD_{cr} = 2\Sigma\varepsilon_T/(\alpha\varepsilon_f) \tag{7}$$

5.3 Plastic tension strain and deformation of CFT-column

The relation between the plastic tension strain (ε_T) and CFT-column deformation (ϕ/ϕ_u) is derived by assuming the following conditions[5].

i) The bending moment of CFT-column distributes linearly along the axis and the curvature in the plastic zone between M_y and M_u also distributes linearly as shown in Fig.13.

ii) The plastic zone does not change according to the column deformation.

The plastic tension strain of steel tube (ε_T) at fixed-end section can be expressed by the curvature of this section(κ_p) as shown in Eq.(8).

$$\varepsilon_T = (1+\cos\theta_n)\frac{D}{2}\kappa_p \tag{8}$$

in which D: diameter of steel tube, θ_n: polar coodinate of neutral axis. From the equilibrium condition of axial force and the stress distribution of CFT-column under ultimate bending moment as shown in Fig.14, Eq.(9) is obtained.

$$\pi(1+\rho)\frac{N}{N_u} - \frac{1}{\sqrt{3}}(3\theta_n - 2\pi) - r\rho(\theta_n - \sin\theta_n\cos\theta_n) = 0 \tag{9}$$

in which N/N_u ($N_u=\sigma_cA_c+\sigma_uA_s$): axial force ratio, r ($=\sigma_{ce}/\sigma_c$, σ_{ce} : strength of confined concrete): confine effect. The confine effect of filled concrete (r) was given by $r=0.76/\rho+0.76$[5] on the basis of CFT-column test. From the conditions i)-ii) mentioned above, the curvature (κ_p) of plastic deformation at the fixed-end can be expressed by the plastic deformation ratio $\mu(=\phi_p/\phi_u)$ in which $\phi_p(=\delta_p/L_c)$: plastic column deformation, L_c: column length as shown in Eq.(10).

$$\kappa_p = \frac{6}{(1-M_y/M_u)(2+M_y/M_u)}\left(\frac{\phi_u}{L_c}\right)\mu \tag{10}$$

Substituting κ_p in Eq.(10) into Eq.(8), ε_T is expressed by μ_T which is the plastic deformation ratio of CFT-column

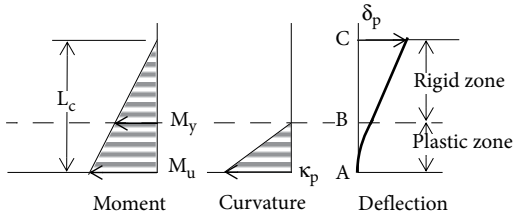

Fig.13 Assumed plastic deformation and moment distribution of CFT-column

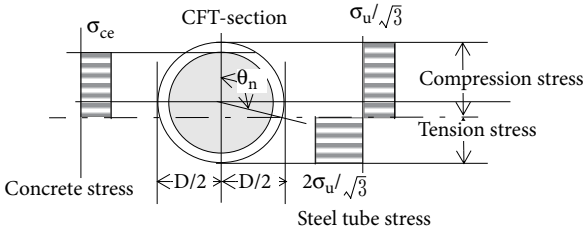

Fig.14 Stress distribution of CFT-column under ultimate bending moment

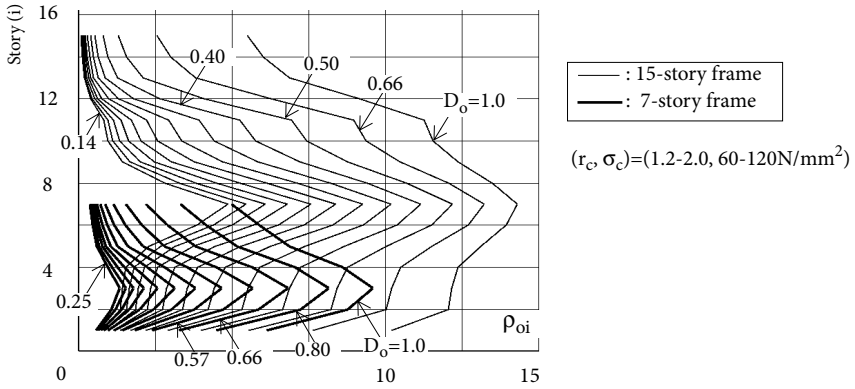

Fig.15 Strength ratio of concrete to steel tube (ρ_{oi}) under optimum design condition to prevent damage concentration

to give the plastic tension strain of steel tube in the tension stress side.

$$\varepsilon_T = f_T \mu_T \qquad \text{in which} \quad f_T = \frac{3(1+\cos\theta_n)}{(1-M_y/M_u)(2+M_y/M_u)}\left(\frac{D}{L_c}\right)\phi_u \tag{11}$$

The accumulated tension plastic strain ($\Sigma\varepsilon_T$) is given by Eq.(12) because f_T in Eq.(11) is not effected by the cyclic load.

$$\Sigma\varepsilon_T = f_T \Sigma\mu_T \tag{12}$$

in which $\Sigma\mu_T$ is the accumulated plastic deformation ratio of CFT-column to give the tension plastic strain of steel tube in the tension stress side. $\Sigma\mu_T$ is nearly equal to the half of the accumlated plastic deformation ($\Sigma\mu_T = \Sigma(\Delta\phi_p/\phi_u)/2$). In section 3.3 the accumulated plastic deformation ($\Sigma(\Delta\phi_p/\phi_u)$) is shown to be approximated by the value of P_i (i: number of story) in Eq.(6). By expressing $\Sigma\mu_T$ by the average value P_{oi} (Fig.11) of P_i, Eq.(13) is obtained.

$$\Sigma(\varepsilon_T)_i = (f_T)_i \frac{P_{oi}}{2} \tag{13}$$

By the use of Eq.(13), the fracture damage ratio of CFT-column $({}_cD_{cr})_i$ in Eq.(2) can be expressed by P_{oi}.

$$({}_cD_{cr})_i = \left(\frac{f_T}{\alpha\varepsilon_f}\right)_i P_{oi} \tag{14}$$

Under the condition that the fracture damage ratio of every story is equal to D_o (D_o: constant), the optimum design condition to prevent the damage concentration of CFT-column can be derived and expressed by Eq.(15).

$$\left(\frac{f_T}{\alpha\varepsilon_f}\right)_i P_{oi} - D_o = 0 \tag{15}$$

5.4 Optimum design condition to prevent damage concentration

Instead of the design condition iii) in section 3.1, the optimum design condition expressed by Eq.(15) is used to design CFT-frames. The strength ratios of concrete to steel tube (ρ_i) of CFT-columns in these designed CFT-frames are also coresponding to the optimum design conditions to prevent the damage concentration of CFT-frame.

The strength ratios ρ_i change in the range smaller than about 10% according to the design condition of CFT-frame. From this reason the strength ratios of concrete to steel tube (ρ_{oi}) as the optimum design condition are given by the average values of ρ_i. The final optimum design condition expressed by the strength ratio of concrete to steel tube (ρ_{oi}) is shown in Fig.15.

6. DAMAGE OF CFT-FRAME UNDER OPTIMUM DESIGN CONDITION

By the use of the optimum design condition given by ρ_{oi}, CFT-frames are designed under the conditions in section 3.1 except the condition iii). The designed CFT-frames are explained by black circles in Fig.7 and compared with the CFT-frames designed without the optimum design condition and shown with white circle in Fig.7. It is shown in Fig.7 that there is not clear difference of the diameter of CFT-column (D) and the natural period (T) among the frames.

In this optimum design of CFT-frame, it is also shown that some CFT-frames can not be designed to satisfy the design condition of ρ_{oi} because the difference among the values ρ_{oi} of all stories are too large. From this reason the CFT-frames to which the optimum design condition of ρ_{oi} is applicable are limited.

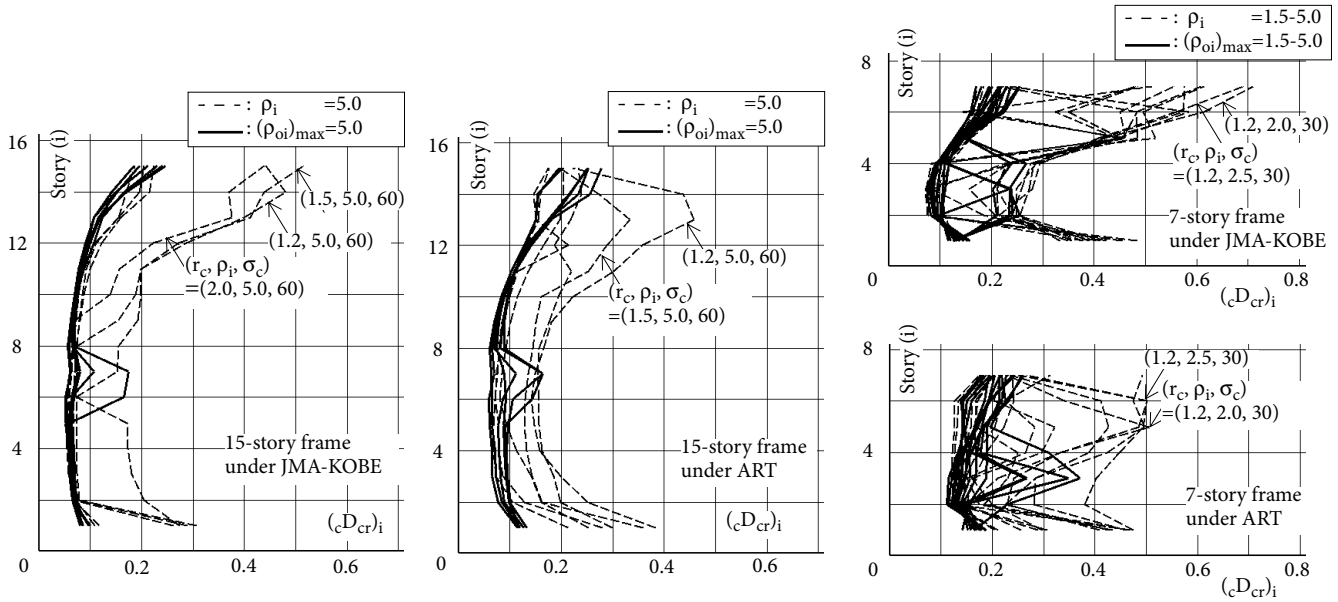

Fig.16 Damage distribution of CFT-frame designed under the optimum design condition to prevent damage concentration

The seismic response damage of these CFT-frames under optimum design condition are shown by real lines in Fig.16. The dashed lines in Fig.16 show the seismic response damage of CFT-frame designed under the same conditions in section 3.1 and without the optimum design condition of ρ_{oi}. Comparing the real lines with the dashed lines, it is ascertained that the damage concentration and the fracture damage ratio of the real lines are small enough and the derived optimum design condition expressed by ρ_{oi} is useful.

7. CONCULSIONS

To prevent the fracture damage concentration of CFT-frame, the design condition expressed by the strength ratio of filled concrete to steel tube of CFT-column is derived. On the basis of numerical analysis of seismic response damage of multi-story CFT-frame, it is ascertained that the proposed optimum design condition to prevent the fracture damage concentration of CFT-column is useful.

REFERENCES

1) Saisho,M., Dynamic Collapse of CFT-Frame under Extremely Strong Ground Motion, *Proceedings of the 13th World Conference on Earthquake Engineering* , Paper No.1877, 2004.8.

2) Saisho,M., Seismic Response and Collapse of Concrete Filled Steel Tube Frame under Extremely Strong Ground Motion, *Proceedings of the 9th Pacific Structural Steel Conference (PSSC2001)*, Vol.1, pp.441-446, 2001.10.

3)Saisho,M.and Kato,M., Damage of Concrete Filled Steel Tube Structure under Extremely Strong Ground Motion, *Proceedings of the 13th European Conference on Earthquake Engineering* , Paper No.775, pp.1-15, 2006.9.

4) Saisho,M. and Goto,K., Ultimate Earthquake Resistant Capacity of CFT-Frame, *Proceedings of the 13th World Conference on Earthquake Engineering*, Paper No.2613, 2004.8.

5) Saisho,M. and Matsuyama,T., Restoring Force Characteristics and Model of Concrete Filled Steel-Tube Column, *Proceedings of the 12th World Conference on Earthquake Engineering*, Paper No.1090, 2000.1.

6) Saisho,M. and Goto,K., Restoring Force Model of Concrete Filled Steel Tube Column under Seismic Load, *Proceedings of the 9th Pacific Structural Steel Conference (PSSC2001)*, Vol.1, pp.453-458, 2001.10.

7) Saisho,M., Kato,M. and Gao,S., Local Buckling of CFT-Column under Seismic Load, *Proceedings of the 13th World Conference on Earthquake Engineering*, Paper No.2614, 2004.8.

8) Clough, R.W. and Johnston,S.B., Effect of Stiffness Degradation on Earthquake Ductility Requirements, *Proceedings of Japan Earthquake Engineering Symposium*, pp.227-232, 1966.10.

9) Dowling, N.E., Mechanical Behavior of Materials, *Prentice Hall*, 1993.

Acknowledgement

This study was supported by the Grant-in-Aids for Scientific Research of Japan No.08455263, No.14550573, No.16560502 and No.20560526.